Towards metal free supported quaternary ammonium halides catalysts for an optimized cycloaddition of CO 2 onto styrene oxide

Miguel Alonso de La Peña, Matthieu Balas, Julie Kong, Richard Villanneau, Lorraine Christ, A. Tuel, Franck Launay

Towards metal free supported quaternary ammonium halides catalysts for an optimized cycloaddition of CO_2 onto styrene oxide

Miguel Alonso de la Peña,[a] Matthieu Balas,[b,c] Julie Kong,[b,c] Richard Villanneau,[b*]
Lorraine Christ,[a] Alain Tuel,[a*] Franck Launay[c*]

a. Université de Lyon, Institut de Recherches sur la Catalyse et l'Environnement de Lyon, UMR CNRS 5256, Université Claude Bernard Lyon 1, 2 av. Einstein, 69626 Villeurbanne Cedex, France. E-mail: alain.tuel@ircelyon.univ-lyon1.fr

b. Institut Parisien de Chimie Moléculaire, CNRS UMR 8232, Sorbonne Université, Campus Pierre et Marie Curie, 4 Place Jussieu, F-75005 Paris, France. E-mail: richard.villanneau@sorbonne-universite.fr.

c. Laboratoire de réactivité de surface, UMR CNRS 7197, Sorbonne Université, Campus Pierre et Marie Curie, 4 Place Jussieu, F-75005 Paris, France. E-mail: franck.launay@sorbonne-universite.fr.

ABSTRACT:

The present work reports on a large selection of porous siliceous materials functionalised by quaternary ammonium salts (QAS) with various pores structures, possible doping with Zn^{2+}, and different ammonium salt substituents as well as halide counter-ions. After characterization by TGA, N_2 physisorption, XRD, XPS and ^{13}C NMR, the latter were tested as catalysts for the cycloaddition of CO_2 onto styrene oxide to produce styrene carbonate. Control experiments performed with the naked silica supports and soluble QAS demonstrated the synergistic action of the silanol groups on the supports and the quaternary ammonium salts. Most importantly it was also shown that covalent grafting confirmed the trend, without reducing the catalytic activity in comparison with conditions where soluble QAS were used. However, the possibility to recycle the entire catalytic system is an obvious benefit of heterogenized QAS. Quite clearly, our work highlighted the higher catalytic efficiency of the most hindered quaternary ammonium salt (butyl groups) combined with bromide ions. The resulting catalysts were tested under three types of conditions: in dichloromethane at 3 mol% at 100°C under 10 bar of CO_2, in benzonitrile at 0.8 mol% at 80°C under 10 bar of CO_2 and in the absence of solvent at 0.2 mol% at 100°C under 20 bar of CO_2. Much better TOF values, of the order of 40 to 50 h^{-1}, were obtained in the latter two cases. Finally, the advantages and disadvantages of these last two catalytic systems are discussed, particularly with regard to the development of a more sustainable chemistry.

Keywords: Quaternary ammonium salts, grafting, CO_2 cycloaddition, solvent-free, mesoporous silica, silanols.

I**NTRODUCTION:** Since the industrial revolution and the emergence of the steam engine, mankind has been constantly meeting a growing need for energy. This energy requires the combustion of fossil fuels, which are abundant on Earth and are considered to be the main source of CO_2 emissions into the atmosphere.[1] This greenhouse gas has always been present and is at the center of many exchanges between the earth's surface, the ocean and the atmosphere via its carbon cycle. However, this balance is disturbed, and a surplus of CO_2 equivalent to 1400 billion tons has since been emitted into the atmosphere between 1850 and 2014.[2] The concentration of CO_2 in the atmosphere has thus reached an all-time high of 416 ppm in 2020, compared to 280 ppm before the industrial revolution.[3]

The reduction of anthropogenic CO_2 emissions is thus an urgent matter and three main strategies are now at work to contain its increasing concentration. The first would be to significantly reduce our energy needs. A second strategy, based on the Carbon Capture and Sequestration (CCS), for example by chemical absorption of CO_2 with amines, is attracting growing interest.[4] The chemical adsorption of CO_2 with amines represents the most mature capture solution to date.[5] Monoethanolamine remains the most currently studied compound for this. Thus obtained CO_2 can for instance be buried in geological faults or used as an abundant renewable and non-toxic C1 carbon resource for the synthesis of high value-added products.[6] The last possibility is referred to as Carbon Capture and Utilization (CCU). It would allow to mitigate CO_2 emissions, but also to slow down the depletion of fossil resources. Although the implementation of CCU remains difficult and time-consuming compared to the CCS strategy, considerable efforts were made in the last two decades. Two main routes have emerged.[7] The one involving the (electro)chemical reduction of CO_2, by converting it to formic acid, carbon monoxide, methane, ethylene or ethanol, is undoubtedly the most studied.[8]

However, the use of CO_2, without modifying the oxidation number of the carbon, also allows access to compounds of very high added value, for example, cyclic carbonates which can be easily obtained by the reaction of CO_2 with epoxides (cycloaddition).[9] It is noteworthy that coupling this reaction with epoxidation in a single pot allows the direct use of alkenes instead of epoxides.[10] In more than 90% of published studies, CO_2 cycloaddition is catalyzed

by quaternary ammonium (QAS) or imidazolium halides with a mechanism involving a Lewis base (LB, the halide) and a Lewis acid (LA, the ammonium or imidazolium cation, which may be coupled to other co-catalysts such as metal complexes).[11]

Very often, soluble QAS are used and, generally, the involvement of electrophilic co-catalysts, among which Zn^{2+} complexes and/or strategies based on the improvement of the nucleophilicity of the Lewis base give rise to more efficient catalytic processes. Recently, it has also been proved that zinc cations can decrease the undesired formation of polycarbonates.[12]

The present manuscript focuses on the use of supported QAS catalysts to improve recyclability and facilitate their separation from the reaction medium, thereby minimizing contamination of the final reaction products. Commercially available anionic polymeric resins bearing quaternary ammoniums salts can be used, but they suffer from low textural parameters and their sensitivity to organic solvents (shrinkage or swelling effects). Furthermore, the comparison of the catalytic efficiency of grafted catalysts onto polymeric resins and silica supports are generally in favor of the latter.[13] We therefore turned to the development of organic/inorganic hybrid materials based on SBA-15 or KIT-6 silicas which have both excellent textural properties and incomparable thermal and solvent resistance. Here, we report our work on mesoporous silicas functionalization using covalent binding of various QAS bearing different alkyl groups and counter-ions. The latter were introduced by the reaction of silica with the corresponding pre-formed silylated QAS precursors. In addition, the prior introduction of Zn^{2+} cations as Lewis acids into the structure of the respective supports was carried out in an attempt to improve the catalytic properties of the resulting materials. Finally, the catalytic activity of all hybrid materials was investigated and compared to that of the corresponding (non-silylated) soluble QAS in the cycloaddition reaction of CO_2. In this context, styrene oxide was chosen here as a benchmark molecule.

EXPERIMENTAL. Solvents and reagents were purchased from commercial sources and used as received except CH_3CN which was purified by classical procedures when mentioned in the text. 3-(trimethoxysilyl)propyl-N,N,N-trimethylammonium chloride and 3-(trimethoxysilyl)propyl-N,N,N-tributylammonium bromide (both 50 % in methanol) were obtained from Alfa Aesar, TCI or ABCR and used as received. Fumed silica Aerosil R812 (280

m^2/g) and precipitated silica Zeosil 175 MP (175 m^2/g) were purchased from Evonik and Solvay respectively. Materials and methods are described in the supplementary information.

1. Silylated-QAS synthesis procedure

As mentioned before, except for commercial 3-(trimethoxysilyl)propyl-N,N,N-trimethylammonium chloride and 3-(trimethoxysilyl)propyl-N,N,N-tributylammonium bromide, the all other QAS (*i.e.* 3-(trimethoxysilyl)propyl-N,N-dimethyl-N'-ethyl ammonium bromide, 3-(trimethoxysilyl)propyl-N-methyl-N',N'-dimethyl ammonium bromide, 3-(trimethoxysilyl)propyl-N,N,N-trimethyl-ammonium bromide, 3-(trimethoxysilyl)propyl-N,N,N-tripropyl-ammonium bromide and 3-(trimethoxysilyl)propyl-N,N,N-tri-$^{n-}$butylammonium iodide) were synthesized.

For the bromide salts, the typical procedure was as follows: 3-bromopropyl trimethoxysilane (BPTMS, 4 mmol) was diluted in 1 mL of dry acetonitrile under N_2 atmosphere. Then, one equivalent of the corresponding amine was introduced dropwise under magnetic stirring. The reaction mixture, was stirred under reflux (82 °C) under N_2 atmosphere during 17 h leading to the quantitative formation of the expected silylated-QAS. After CH_3CN evaporation from the obtained yellow solution, the purity of the target compound was checked by ^1H NMR. The spectroscopic characterization of these compounds was in accordance with the data obtained from the literature.[14]

The N,N,N-tri-$^{n-}$butylammonium iodide ($(MeO)_3Si(CH_2)_3NBu_3I$) was prepared using a slightly modified protocol by mixing tributyl amine ($^{n-}Bu_3N$, 38.5 mmol) and (3-iodopropyl)trimethoxysilane (IPTMS, 25.7 mmol) in dry acetonitrile and stirring the mixture at reflux (82°C) for 17h under N_2 atmosphere. Then the crude mixture was washed with toluene (2x10 mL) and the product dried under vacuum (25.4 mmol, 99%). ^1H NMR ($CDCl_3$, 400MHz): δ = 3.59 (s, 9H), 3.40-3.36 (m, 2H), 3.36-3.32 (m, 6H), 1.85-1.78 (m, 2H), 1.74-1.66 (m, 6H) 1.51-1.42 (m, 6H), 1.02 (t, J=7.34 Hz, 9H), 0.75 (t, J=7.44 Hz, 2H) ppm.

2. Synthesis of the mesoporous silicas

2.1 Synthesis of SBA-15 and KIT-6. SBA-15 silica with a hexagonal *P6mm* phase was prepared according the literature,[15] by acidic hydrolysis of tetraethyl orthosilicate (TEOS) in the presence of Pluronic® P123 (see figure 1) followed by a 24h hydrothermal treatment at

130°C. After filtration and drying, calcination was carried out in air by increasing temperature by 1°C/min from room temperature to 550 °C and maintaining this temperature for 6h.

In a similar way, KIT-6 mesoporous silica with a cubic *Ia3d* phase was obtained by adding ^{n}BuOH (see figure 1).[16] First, Pluronic® P-123 (8 g) was dissolved in a mixture of water (289 mL) and HCl 37% (12.7 mL) at 35 °C. Then, ^{n}BuOH (9.9 mL) was introduced. After stirring for 1h at 35°C, TEOS (18.4 mL, 83.0 mmol) was added and the mixture stirred for 24h at 35 °C. After that, the mixture was heated at 100°C for 24h under static conditions and then the silica was filtered. Silica was washed with water until obtaining a neutral pH and dried in an oven at 120°C for 2h. Calcination was carried out in air by increasing temperature by 1°C.min^{-1} from room temperature to 550°C and maintaining this temperature for 6h.

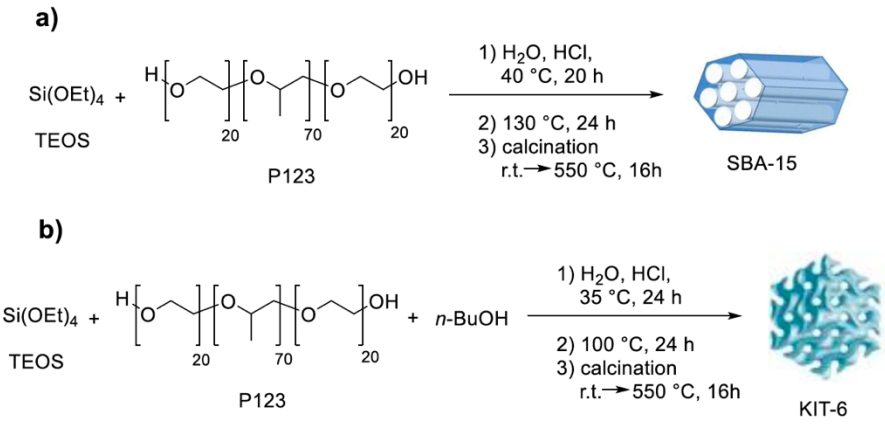

Figure 1. Schematic representation illustrating the preparation of SBA-15 (a) and KIT-6 (b) silica supports.

2.2 Synthesis of Zn/SBA-15 and Zn/KIT6. In parallel, Zn-doped mesoporous silicas were synthesized by adding $Zn(NO_3)_2$ in the synthesis gel. Following a reported work, Zn/SBA-15 was obtained by drying the suspension recovered after the hydrothermal treatment of the synthesis gel containing 0.12 mol of Zn per mol of TEOS.[17] Hence, Pluronic® P-123 (8 g) was dissolved in a mixture of water (260 mL) and HCl 37% (40 mL) at 40°C. Once Pluronic® P-123 was dissolved, $Zn(NO_3)_2.6H_2O$ (2.91 g, 9.79 mmol) was added. After stirring for 0.5h, TEOS (18.1 mL, 81.6 mmol) was introduced and the mixture stirred for 24h at 40°C. After that, the mixture was heated at 100°C for 24h under static conditions and evaporated at 80°C for 18 h under stirring.

Following that, a new material Zn/KIT-6, could be prepared by merging the synthetic paths of KIT-6 and Zn/SBA-15, *i.e.* by adding *n*-BuOH to Zn/SBA-15 synthesis. Pluronic® P-123 (8 g) was dissolved in a mixture of water (289 mL) and HCl 37% (12.7 mL) at 35°C. Once

Pluronic® P-123 was dissolved, $Zn(NO_3)_2.6H_2O$ (2.93 g 9.86 mmol) and ^{n}-BuOH (9.9 mL) were added. After stirring for 1h at 35°C, TEOS (18.4 mL, 82.1 mmol) was added and the mixture stirred for 24h at 35°C. After that, the mixture was heated at 100°C for 24h under static conditions and evaporated at 80 °C for 18h under stirring.

Calcination in both cases was carried out in air by increasing temperature by 1°C/min from room temperature to 550°C and maintaining this temperature for 6h. Zn loadings for Zn/SBA-15 and Zn/KIT-6 obtained by ICP-AES (Inductively Coupled Plasma Atomic Emission Spectroscopy) were 9.7 wt.% and 9.6 wt.%, respectively (expected value: 11%).

3. Procedure for silylated-QAS grafting onto silica supports [max. 2 mmol.g^{-1}]: The procedure was adapted from the literature, with slight differences depending on the supports.[18]

3.1 Silylated-QAS grafting onto SBA-15. SBA-15 was vacuum dried at 120°C for 3 h. After cooling to room temperature, 10 mL of anhydrous toluene were added per gram of SBA-15 placed under N_2 atmosphere in a two-necked vessel connected to a condenser. The resulting suspension was immerged in an ultrasonic bath for 15 min. Then, under stirring, 2 mmol of QAS (per gram of SBA-15) were added dropwise. The suspension was stirred at room temperature for 2h and then, heated in refluxing toluene for 24h. The white solid was recovered by filtration on glass frit (porosity 4), washed with acetone and CH_2Cl_2 using a Soxhlet. The obtained material was dried overnight at 50°C and vacuum dried for 5h.

3.2 Silylated-QAS grafting onto other supports. Blank experiments were also carried out with commercially available silicas such as fumed silica Aerosil R812 (Aerosil 300 treated with hexamethyldisilazane, a trimethylsilylating agent converting -OH groups into $-OSiMe_3$ (280 $m^2.g^{-1}$)) and precipitated silica Zeosil 175 MP (175 $m^2.g^{-1}$), purchased from Evonik and Solvay, respectively. Firstly, the silica support was hydrolyzed in boiling water for 2h. After filtration, silica was dried at 135°C for 16h, then dispersed in toluene (1.00 g of support for 100 mL of toluene). The required amount of $(MeO)_3Si(CH_2)_3NR_3X$ in 50% methanol (targeting 2mmol per gram of support) was added and the mixture was stirred 8h at room temperature and 16h at reflux (111°C). After filtering (glass frit porosity 4), silica was washed with toluene (3x30 mL) and dichloromethane (3x30 mL), then dried under vacuum for 5h.

4. Catalytic cycloaddition of CO_2 on styrene oxide:

4.1 Preliminary catalytic tests with inorganic supports and soluble QAS. In a typical reaction, 0.06 mmol (3 mol.%) of halide ammonium salt (QAS), styrene oxide (0.230 mL, 2 mmol) and mesitylene (0.14 mL, 1 mmol), used as internal standard, were placed into a 40 mL stainless steel reactor. Dichloromethane was added before closing and pressurizing the reactor with CO_2 (P_{ini} = 10 bars) then the reactor was heated to the desired temperature during 6h. Later, the reactor was cooled down to room temperature in an ice bath before depressurizing. The final reaction mixture was filtered and the organic fraction was analyzed by ^1H NMR (300 µL of sample using filter membranes were diluted in 700 µL of $CDCl_3$). In some tests, SBA-15, KIT-6, Zn/SBA-15 and Zn/KIT6 were also introduced.

4.2 Catalytic tests using {$R_3N^+X^-$}@SBA-15 with optimized conditions. Styrene oxide (0.670 mL, 5.6 mmol), 20 mL of benzonitrile, {$R_3N^+X^-$}@materials (corresponding to *c.a.* 0.045 mmol of QAS, 0.8 mol.%) and 8.0 mmol of *p*-xylene (1 mL), used as internal standard, were introduced in a 40 mL Teflon vessel. The resulting suspension was stirred for 5 min at room temperature and then pressurized in a stainless-steel autoclave with 10 bar of CO_2 before heating to 80 or 120°C for 3 or 23 h with a temperature increase of 2.5 °C.min^{-1}. The autoclave was then cooled down at room temperature using an ice bath and the reaction medium analyzed by GC-FID, after filtration.

4.3 Catalytic tests under solvent-free conditions. In a typical reaction, {$R_3N^+X^-$}@materials (corresponding to 0.06 mmol of halide, 0.2 mol.%) and styrene oxide (3.5 mL, 31 mmol) were directly placed into the autoclave, which was closed and pressurized with 20 bar of CO_2 (corresponding to 32 mmol of CO_2) then heated at 100°C for 6h. When the experiment was completed, mesitylene (0.28 mL, 2 mmol) was added as internal standard. The organic layer of the crude mixture was extracted with 5 mL of CH_2Cl_2 and then filtered. Samples were analyzed by NMR (200 µL diluted in 800 µL of $CDCl_3$). Then, the powder recovered by filtration was washed with CH_2Cl_2 (8x10 mL) in order to analyze the lixiviation of QAS by TGA.

4.4. Catalyst recycling tests. Reuse tests were carried out using the same procedure as for a standard catalytic test under solvent-free conditions (see paragraph 4.3). Thus, {$Bu_3N^+Br^-$}@SBA-15 (95.9 mg, corresponding to 0.06 mmol of halide, 0.2 mol.%) and styrene oxide (3.5 mL, 31 mmol) were placed in the autoclave. The autoclave was then pressurized with 20 bar of CO_2 and heated to 100 °C. After 6 h, the reactor was cooled down in an ice

bath, depressurized and mesitylene (0.28 mL g, 2 mmol), dissolved in 5 mL of CH_2Cl_2, was added as standard for NMR analysis. The catalyst was then filtered and washed with CH_2Cl_2. After drying the recovered powder under vacuum, a new run was carried out by adding a new amount of styrene oxide calculated based on the catalyst mass remaining after recovery in order to keep constant the SO/catalyst molar ratio throughout the series of recycling experiments.

RESULTS AND DISCUSSION

5. Synthesis and characterization of the materials

5.1 General strategy. Silica supported organic functions are generally introduced either *i)* in the synthesis gel, with the silica precursors ("co-condensation pathway") or *ii)* by post-functionalization of the pre-formed inorganic support ("post-synthesis pathway"). In all cases, quaternary ammonium halides bearing trialkoxysilylane groups are necessary. In the present work, SBA-15 and KIT-6 were prepared upstream and reacted, in a second step, with the organosilane precursors with QAS terminations ("post-synthesis pathway"). The scope of commercially available quaternary ammonium salts bearing trialkoxysilylane groups is however limited. Conventional QAS synthesis procedures used in organic chemistry are generally based on the reaction of halogenoalkyl derivatives with tertiary amines. Such syntheses can be performed either before grafting the silylated QAS molecule (*ex-situ* grafting strategy, see Scheme 1) or, in two steps, by initial grafting of a halogeno-alkyl derivative onto the support, then reaction of this pre-anchored grafted molecule with the targeted tertiary amine (*in-situ* grafting strategy, see Scheme 1). These two synthetic methods were largely illustrated in the literature, whether with silica or other types of supports. However, the performances of such materials in which organic cations are covalently grafted were hardly evaluated as catalysts for the CO_2 cycloaddition on epoxides.[19] To date, only one example using QAS-functionalized silica support as catalyst for this reaction was described in the literature, to our knowledge.[20] In the present work, an *ex-situ* strategy was preferred since it displays several advantages. Indeed, such procedure allows to characterize the silylated quaternary ammonium halide precursors before grafting, in homogeneous phase, and to purify them, if necessary, using molecular chemistry techniques. Secondly, it also ensured uniform surface functionalization by only allowing grafting of the target molecule. In the other method, non-post-functionalized sites may remain on the

surface of the materials. Third, the choice of halide containing QAS, rather than other salts classically used for the cycloaddition reaction, was finally justified by the great flexibility in their synthesis. It was thus possible to finely modulate, substituent by substituent, the steric hindrance around the nitrogen atom of the ammonium and its Lewis acid character.

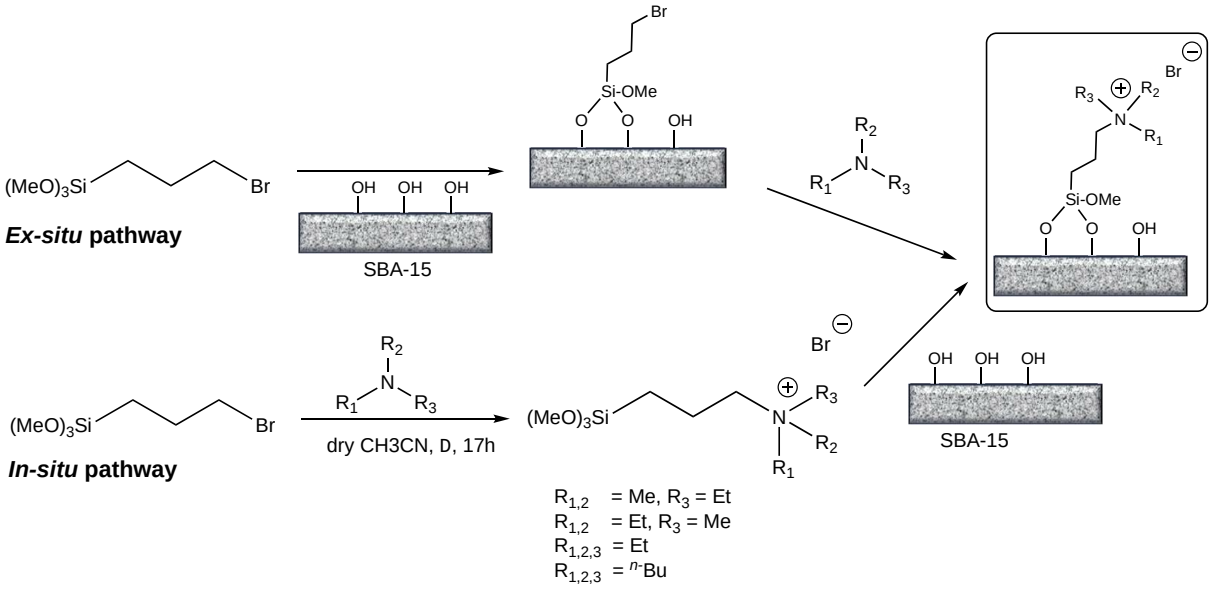

Scheme 1: Preparation of QAS-functionalized SBA-15.

5.2 Synthesis and characterization of the molecular silylated QAS precursors. The synthesis of the non-commercial silylated quaternary ammonium was carried out by the reaction of (3-bromopropyl)trimethoxysilane (BPTMS) or of (3-iodopropyl)trimethoxysilane (IPTMS) with the corresponding tertiary amine. Among the different solvents (MeCN, toluene, THF) and reaction temperatures tested, refluxing dry MeCN (see experimental conditions) led to the best results for the synthesis of the triethylammonium derivative $[(MeO)_3SiCH_2CH_2CH_2NEt_3]^+Br^-$ which was used as model compound for optimizing the synthesis conditions. However, reaction of NEt_3 with 3-chloropropyl trimethoxysilane (CPTMS) did not lead to a significant yield in the corresponding ammonium, due to the poorer leaving group ability of chloride compared to bromide. The compounds bearing $\{Me_2EtN^+Br^-\}$, $\{Et_2MeN^+Br^-\}$, $\{Et_3N^+Br^-\}$, $\{^{n-}Bu_3N^+Br^-\}$ or $\{^{n-}Bu_3N^+I^-\}$ terminations were thus prepared using BPTMS and/or IPTMS with almost complete yields (from 92 to 99 % based on ^1H NMR analysis) within 17 h. The compound bearing a $\{Pr_3N^+Br^-\}$ group (see Table S1 for details) was also prepared but in a rather low yield (42%). In this last case, it was not possible to separate properly the ammonium from unreacted amine or BPTMS, and it was not used for further grafting on silica.

Characterization of the mesoporous supports. The four porous supports (SBA-15, Zn/SBA-15, KIT-6 and Zn/KIT-6) were first characterized by powder X-Ray Diffraction (XRD, see supplementary materials, figures S1 and S2). The aim of this technique was not only to confirm the pore arrangement but also to observe whether Zn atoms were dispersed or, on the contrary, forming zinc oxide aggregates in the Zn-doped materials. Both SBA-15 and Zn/SBA-15 mesoporous materials provided similar XRD patterns at low angle (Figure S1.a). Therefore, they are characterized by the same pore arrangement, displaying characteristic (100), (110), and (200) diffraction peaks typical of a lamellar 2D p6 mm hexagonal structure. The same analysis was carried out for KIT-6 and Zn/KIT-6, affording similar results. At low angle (Figure S2.a), the two materials provided similar patterns indicating the same pore organization corresponding to a cubic 3D Ia3d pore network. In addition, the lack of zinc oxide patterns in standard XRD for Zn/SBA-15 and Zn/KIT-6 (Figures S1.b and S2.b) revealed that Zn atoms were totally dispersed. N_2 sorption isotherms were also carried out in order to obtain more information about the surface and the porosity of the SBA-15, Zn/SBA-15, KIT-6 and Zn/KIT-6 solids. Isotherms were rather similar (see figure S3) and corresponded to type IV, according to IUPAC classification.[21] Moreover, the hysteresis of H1 type obtained with the four materials pointed out the presence of a range of uniform mesopores. All the materials have in common a narrow pore size distribution centered around 6-7 nm (see Table 1).

Table 1. *Textural characteristics of SBA-15, Zn/SBA-15, KIT-6 and Zn/KIT-6*

Sample	Zn ($mmol.g^{-1}$)	S_{BET} ($m^2.g^{-1}$)	Pore Vol. ($cm^3.g^{-1}$)	Average Pore diameter (nm)
SBA-15	-	900	1.12	6.2
Zn/SBA-15	1.48	567	0.86	6.1
KIT-6	-	860	1.12	6.5
Zn/KIT-6	1.47	678	0.94	7.1

5.3 Grafting of silylated-QAS and characterization of the resulting materials. The silylated QAS were then grafted on SBA-15, Zn/SBA-15, Kit-6 and Zn/Kit-6, as well as commercial Zeosil used for comparison targeting the corresponding $\{R_3N^+X^-\}$@support materials. The optimized experimental procedure involved i) prior activation of the supports by drying in vacuum at high temperature and ii) grafting in refluxing toluene for a long

period. All the corresponding materials were characterized by XRD, Thermogravimetric analyses (TGA), X-ray fluorescence (XRF) and study of their textural properties.

Grafting of the $[(MeO)_3SiCH_2CH_2CH_2NR_3]^+X^-$ precursors onto SBA-15. The QAS content of the $\{R_3N^+X^-\}$@SBA-15 materials was estimated using TGA and XRF measurements (see supplementary information for the calculation method, figure S4). In the case of XRF, 3 calibration curves for Zn were performed by supporting zinc halides ($ZnCl_2$, $ZnBr_2$ and ZnI_2) on silica (see supplementary information for details). All data are summarized in Table 2. QAS loading (expected 2 mmol.g^{-1} of support) was roughly found to be inversely proportional to chain length and the size of the halide, *i.e.* from *ca.* 2 mmol.g^{-1} for $\{Me_3N^+Cl^-\}$@SBA-15 to 0.68 mmol.g^{-1} $\{Bu_3N^+I^-\}$@SBA-15. It seems that the surface concentration of -NMe_3^+-terminated QAS was significantly higher than with the other synthons.

Grafting of the Si-QASs onto SBA-15 did not affect the hexagonal pore structure of the support as indicated by the systematic presence of the XRD peaks corresponding to the (100), (110) and (200) reticular planes characteristic of SBA-15 (see Figure **S5,** top right). An overall decrease of the specific surface (S_{BET}) as well as of the pore volume and average pore diameter was observed after grafting. For sake of illustration, the final values of S_{BET} were in the range of 262 m^2.g^{-1} for $\{Me_3N^+Cl^-\}$@SBA-15, which has the highest QAS loading, to 433 m^2.g^{-1}, in the case of $\{Me_2EtN^+Br^-\}$-SBA-15 (**Table 2**). These tendencies were expected and obviously compatible with the incorporation of silylated organic groups inside the pores of the SBA-15 support.[22]

Table 2. *Textural characteristics and QAS loadings of the $\{R_3N^+X^-\}$@SBA-15 materials*

Sample	S_{BET} (m^2.g^{-1})	Average Pore diameter (nm)	Organic function loading		
			Molar conc. (mmol.g^{-1})*	wt.%X (TGA)	wt.%X (XRF)
SBA-15	900	6.2	*N/A*		
$\{Me_3N^+Cl^-\}$@SBA-15	262	5.7	2.03	7.2	8.9
$\{Me_2EtN^+Br^-\}$@SBA-15	433	5.3	1.26	10.1	9.8
$\{Et_2MeN^+Br^-\}$@SBA-15	320	5.6	1.17	9.4	9.7
$\{Et_3N^+Br^-\}$@SBA-15	415	5.3	1.22	9.7	6.8
$\{Bu_3N^+Br^-\}$@SBA-15	381	5.6	0.74	5.9	5.3
$\{Bu_3N^+I^-\}$@SBA-15	355	5-6	0.68	8.6	9.9

** Estimated from TGA measurements.*

X-ray photoelectron spectroscopy (XPS) analysis was also performed on three $\{R_3N^+X^-\}$@SBA-15 materials. In all cases, the bromine signal (Figure **2**, top) could be deconvoluted in the Br $3d_{3/2}$ (69.2 eV) and Br $3d_{5/2}$ (68.1 eV) components ascribed to Br^-.[23] For nitrogen, the main peak observed at 400.8 eV (N 1s) was that expected for a quaternary ammonium, but a much smaller one at 398.0 eV was also visible, revealing the presence of 2 types of nitrogen. Given that the $\{R_3N^+X^-\}$ precursors were not purified before the grafting step, the additional N peak in the three XPS spectra was attributed to the presence of a small amount of non-reacted tertiary amine. Nevertheless, the XPS molar ratio between ammonium-type nitrogen atom and bromide was found close to 1 (from 0.9 to 0.97).

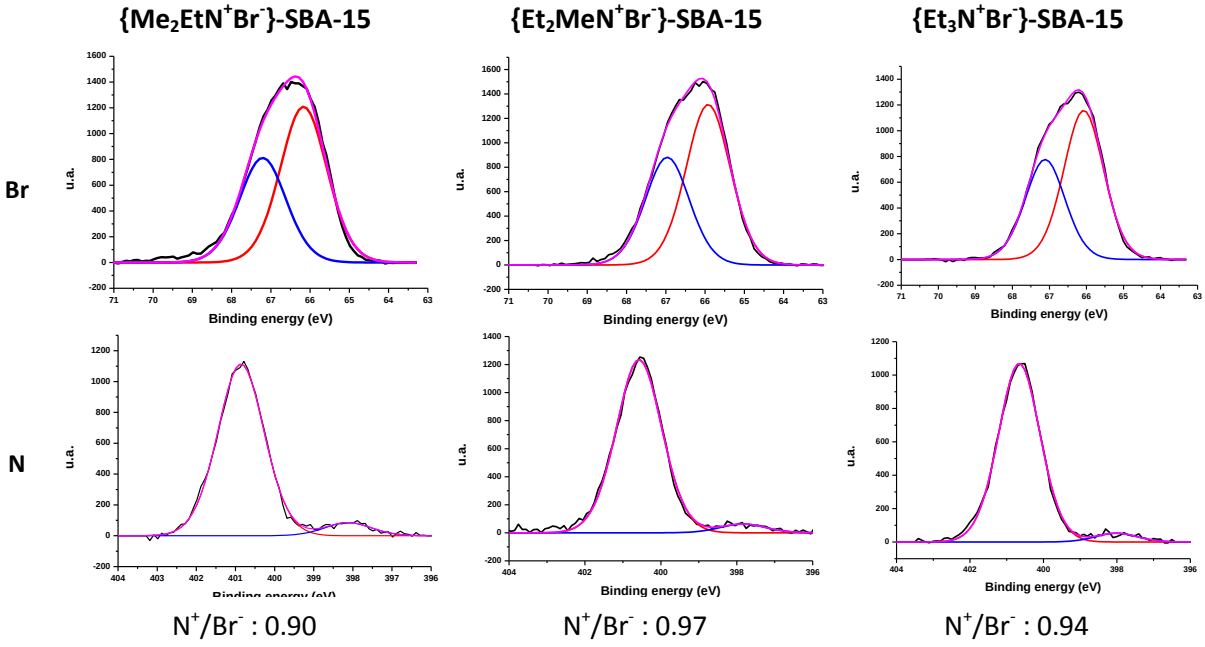

Figure 2: XPS analysis of bromine and nitrogen elements of three $\{R_3N^+X^-\}$@SBA-15 materials.

To assess the covalent grafting of ammonium halides, the solids were analyzed by ^{1}H-^{29}Si CP-MAS (Cross polarization - Magic Angle Spinning) NMR technique. Such analysis is not quantitative since silicon atoms far from protons do not benefit from magnetization transfer and are therefore not detected. However, the evolution of surface species upon grafting (decrease of the signal corresponding to silanol groups) is a good indication of the grafting and can be used as a semi-quantitative estimation of the amount of grafted moieties. For illustrative purposes, the ^{1}H-^{29}Si CP-MAS spectra of $\{Bu_3N^+Br^-\}$@SBA-15 and neat rehydrated silica SBA-15 are shown Figure 3. As expected, silica provided three peaks between -80 and -120 ppm corresponding respectively to Q_4 ($\underline{Si}(OSi)_4$), Q_3 (HO-$\underline{Si}$-$(OSi)_3$) and Q_2 $(HO)_2$-$\underline{Si}$-$(OSi)_2$)

species. In the spectrum of $\{Bu_3N^+Br^-\}$@SBA-15, peaks corresponding to siloxane (R-Si-$(OSi)_x(OH)_y$) species were observed around -60 ppm, apart from those ones related to silicates (Q_4, Q_3 and Q_2). The grafting of QAS functions was also evidenced by the decrease of Q_2 and Q_3 with respect to Q_4.

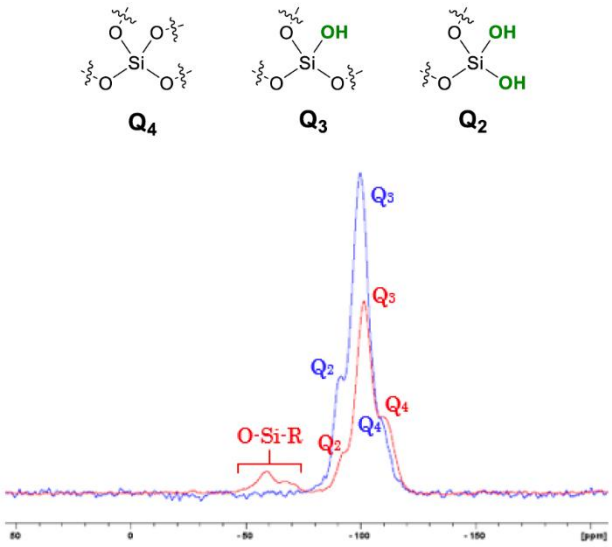

Figure 3. ^1H-^{29}Si CP-MAS NMR spectra of neat SBA-15 (in blue) and $\{Bu_3N^+Br^-\}$@SBA-15 (in red).

Comparative grafting of $[(MeO)_3SiCH_2CH_2CH_2NBu_3]^+Br/I^-$ on different supports.

With soluble QAS, it has often been reported that factors increasing the nucleophilicity of halides, including steric hindrance induced by the nitrogen atom alkyl substituents, have a positive effect on the catalytic performance in cycloadditions. Consequently, the silylated QAS precursors with the butyl groups (*i.e.* $[(MeO)_3SiCH_2CH_2CH_2NBu_3]^+Br/I^-$) were chosen in order to systematically study the effect of the support on the catalytic efficiency of QAS after immobilization. Both QAS were thus covalently grafted onto all supports prepared during the course of this study and onto a commercial Zeosil, used as a reference. The targeted amount of grafted QAS was 2 $mmol.g^{-1}$. The textural characteristics and QAS loadings of the $\{Bu_3N^+X^-\}$@support materials are displayed in Table 3. Since QAS grafting is strongly dependent on the number of silanols available, Zeosil provided the lowest halide loadings per gram of support due to its significantly smaller surface area (see Table 1). Except Zeosil, all other materials displayed equivalent specific surfaces, in the range of 310 to 381 $m^2.g^{-1}$. Furthermore, for similar supports, the general trend observed was that, for the same supports, the bromide concentration was slightly higher overall than the iodide content. Similar Zn loadings were also obtained with the two materials containing iodides, $\{Bu_3N^+I^-\}$@Zn/SBA-15 and $\{Bu_3N^+I^-\}$@Zn/KIT-6 (respectively 1.28 and 1.39 $mmol.g^{-1}$) which is a little

lower than 1.47 and 1.48 for the corresponding supports (Table 1). However, for Zn/SBA-15 and Zn/KIT-6, intriguing behavior was observed since low Zn^{2+} contents were observed, especially for {$Bu_3N^+Br^-$}@Zn/SBA-15 (0.11 mmol.g^{-1}). It seemed that bromide favored lixiviation of the Zn^{2+} from the SBA-15 silica support. However, this was not to the detriment of the QAS content within the material, which remained in the average range of those observed in other materials Nevertheless, no appreciable Zn leaching was observed for Zn/SBA-15 when using ammonium iodide.

Table 3. *Textural characteristics and QAS loadings of the {$Bu_3N^+X^-$}@support materials*

Sample	S_{BET} ($m^2.g^{-1}$)	Average Pore diameter (nm)	Elemental loading (mmol.g^{-1})		
			Zn (XRF)	X (TGA)	X (XRF)
{$Bu_3N^+Br^-$}@Zeosil	148	20-60	-	0.33	0.28
{$Bu_3N^+I^-$}@Zeosil	136	10-50	-	0.31	0.28
{$Bu_3N^+Br^-$}@SBA-15	381	5-6	-	0.74	0.70
{$Bu_3N^+I^-$}@SBA-15	355	5-6	-	0.67	0.78
{$Bu_3N^+Br^-$}@Zn/SBA-15	355	5-6	0.11	0.83	0.94
{$Bu_3N^+I^-$}@Zn/SBA-15	366	5-6	1.39	0.67	0.63
{$Bu_3N^+Br^-$}@KIT-6	380	4-6	-	0.91	1.06
{$Bu_3N^+I^-$}@KIT-6	348	4-6	-	0.80	0.96
{$Bu_3N^+Br^-$}@Zn/KIT-6	362	5-7	0.92	0.74	1.06
{$Bu_3N^+I^-$}@Zn/KIT-6	316	5-6	1.28	0.61	0.69

As a conclusion of this part, XRD, TGA, XPS analyses and N_2 physisorption measurements on the different materials grafted with silylated QAS precursors showed that there is no degradation of the silica support. The concomitant reduction of the specific surface area, of the average pore diameter and of the pore volume are good indicators showing that the grafting took place homogeneously within the pores of all materials as expected. Furthermore, all QAS-functionalized silicas provided similar results for halide loading per square meter of surface area, between 1.5 and 2.9 μmol.m^{-2}, highlighting that the main factor was the specific surface area and not the intrinsic structure of silica.

6. Catalytic performances towards CO_2 cycloaddition onto styrene oxide

6.1. Comparison of {$Bu_3N^+X^-$}@materials with soluble $Bu_4N^+X^-$ in the presence of the naked supports. Soluble QAS considered individually have demonstrated fairly good catalytic activity for the cycloaddition of CO_2, even at industrial scale, but at rather high temperatures

and pressures. These reaction conditions can be lowered by coupling to these QAS co-catalysts acting as Lewis acids, *i.e.* capable of activating the opening of the oxirane ring. Among these, molecules capable of forming H bonds have been used extensively. Hydroxyl groups, such as silanols on the surface of silica, can also contribute in this way. Indeed, the beneficial effect of adding silica or Zn-doped silicata, without ammonium grafts, on the performance of soluble QAS for the cycloaddition of CO_2 to epoxides was documented several times in the literature.[24] The aim of the present preliminary tests was to verify that this effect could be generalized to different types of materials, including those incorporating Zn^{2+}, also acting as a potential additional Lewis acid. Here, unfunctionalized mesoporous silicas (SBA-15, Zn/SBA-15, KIT-6 and Zn/KIT-6) were tested in the cycloaddition of CO_2 to styrene oxide (SO), in the presence of three tetrabutylammonium halides (NBu_4X, X= Cl, Br and I) used as Lewis bases (LB) (Table 4). The amount of Zn-doped silica (Zn/SBA-15 and Zn/KIT-6) was calculated in order to add 1 mol% of Zn and it was decided that the same mass would be added in the case of neat silicas (SBA-15 and KIT-6). Concerning Lewis bases, a catalyst loading of 3 mol% was used in each experiment, in accordance with previous works done by some of us.[25] To better emphasize the possible effects of the presence of the added solids, all the catalytic tests were performed at 100°C for 6 h under 10 bar of CO_2 and using CH_2Cl_2 as solvent. It has to be also noted that styrene carbonate (SC) selectivity found in each experiment was higher than 93%.

Table 4. *Influence of added silicas or Zn-doped silicas onto NBu_4X catalysed CO_2 cycloaddition*

Entry	Silica	LB (NBu_4X)	SO Conv. (%)	SC Yield (%)
1	-	Cl	9	9
2	-	Br	7	7
3	-	I	6	6
4	SBA-15	Cl	50	47
5		Br	52	50
6		I	49	46
7	Zn/SBA-15	Cl	58	54
8		Br	55	52
9		I	55	54
10	KIT-6	Cl	37	37
11		Br	38	37
12		I	36	35
13	Zn/KIT-6	Cl	45	45
14		Br	42	40
15		I	54	52
16	Aerosil R812	Br	25	25

Reaction conditions: CH_2Cl_2 (5 mL), SO (2 mmol), LB= 3 mol% vs. SO (0.06 mmol), 100°C, P_{CO2}: 10 bar, m_{Silica} = 13.4 mg, 6 h.

Tetrabutylammonium halides alone were tested first under the chosen conditions, affording yields below 10% (Entries 1-3, Table 4). Interestingly, a dramatic increase of the SC yield was systematically observed upon the addition of the different silicas or Zn-doped silicas (Entries 4-15, Table 4). This is particularly important as no trace of styrene carbonate formation could be detected with these materials alone. It is noteworthy, that, for each solid, the SC yields did not depend strongly on the type of halides used. Besides, the activity of the catalytic systems involving the materials with a 2D pore arrangement, *i.e.* SBA-15 and Zn/SBA-15 (Entries 4-9, Table 4), turned out to be higher than that of their respective analogous with a 3D pore arrangement, KIT-6 and Zn/KIT-6 (Entries 10-15, Table 4). Furthermore, it seems that the presence of Zn in the structure slightly enhanced the conversions and yields (Zn/SBA-15 > SBA-15; Zn/KIT-6 > KIT-6). All put together, it happened that the highest yields (54-52%, Entries 7-9, Table 4) was provided by combining mesoporous silica Zn/SBA-15 with any tetrabutylammonium halide (Cl, Br or I). Finally, to provide a definitive proof of the importance of the presence of silanol groups acting as Lewis acids, a commercially available hydrophobic silica, namely Aerosil R812, was tested along with NBu_4Br. As expected, partial trimethylsilylation of its silanols led indeed to significantly lower values of the SO conversion (25%) and SC yield (25%) (Entry 16, Table 4) than those obtained with previous silicas.

The catalytic performances of the bromide and iodide-based $\{Bu_3N^+X^-\}$@materials were also evaluated in the same experimental conditions (See Table 5). Again, all catalysts provided significantly higher SO conversions (33-50%) and SC yields (33-49%) compared to the corresponding soluble tetrabutylammonium halides, which gave 7% (with Br^-) and 6% (with I^-) SC yield respectively (Entries 2 and 3, Table 4). In details, SBA-15 and Zn/SBA-15 silica, with 2D symmetrical pores arrangement (Entries 3-6, Table 5), provided slightly higher results in terms of conversions and yields than the other ones (Zeosil, Entries 1-2 or KIT-6 and Zn/KIT-6 Entries 7-10, Table 5).

Table 5. *Catalytic performances of $\{Bu_3N^+X^-\}$@materials in CO_2 cycloaddition in CH_2Cl_2*

Entry	Silica	SO Conv. (%)	SC Yield (%)
1	$\{Bu_3N^+Br^-\}$@Zeosil	35	35
2	$\{Bu_3N^+I^-\}$@Zeosil	42	42

3	{$Bu_3N^+Br^-$}@SBA-15	50	49
4	{$Bu_3N^+I^-$}@SBA-15	44	43
5	{$Bu_3N^+Br^-$}@Zn/SBA-15	38	37
6	{$Bu_3N^+I^-$}@Zn/SBA-15	43	42
7	{$Bu_3N^+Br^-$}@KIT-6	41	41
8	{$Bu_3N^+I^-$}@KIT-6	38	38
9	{$Bu_3N^+Br^-$}@Zn/KIT-6	33	33
10	{$Bu_3N^+I^-$}@Zn/KIT-6	41	38

Conditions: CH_2Cl_2 (5 mL), SO (2 mmol), LB= 3 mol% vs. SO (0.06 mmol), 100°C, P_{CO2}: 10 bar, m_{Silica} Reaction = 13.4 mg, 6 h

On the other side, it is difficult to assess the influence of the nature of the associated counterion (Br^- vs I^-) or the presence of Zn^{2+} ions in the materials, as the results obtained are relatively close to each other. However, from the comparison of the data in the tables 4 and 5, it seems that grafting of QAS onto Zn-doped silicas is detrimental to the co-catalytic effect of Zn^{2+}. Finally, although the effect of covalent grafting of QAS did not appear so obvious under these experimental conditions at first glance, it helps to obtain heterogeneous catalytic systems, justifying further work. Here, it should be noted that the highest catalytic activity (SO conversion: 50%, SC yield: 49%) was obtained after grafting {$Bu_3N^+Br^-$} ammonium onto SBA-15. Regarding these encouraging results, efforts were done in optimizing the experimental conditions in order to increase SC yield all by using milder conditions.

6.2. Optimization of the experimental conditions for a greener process. A systematic study of the experimental conditions was undertaken in order to optimize the CO_2 cycloaddition onto styrene oxide. The criteria applied aimed to meet as much as possible green chemistry requirements by:

- increasing the ratio between the catalyst and the SO substrate;

- avoiding the use of halogenated solvents and working in free-solvent conditions or at least replacing them by more sustainable solvents, such as nitriles.[26]

- reducing the reaction temperature and/or the reaction time.

- studying the parameters likely to improve the efficiency of the catalyst.

In fine, two sets of reaction parameters were therefore retained in this study (see paragraphs 6.2.1 and 6.2.2 beside) because they met, at least in part, these different criteria, while making it possible to improve the performance of the catalysts studied.

6.2.1. Effect on the chain length of the grafted QAS. As detailed before, the intrinsic nature of the support and of the halide associated to the grafted QAS had moderate effect on the yield of the catalytic reaction, using the previous set of reaction parameters. In this part, we have focused our attention on the impact of the steric hindrance on the nitrogen atom of grafted QAS. Based on the best results obtained so far (entry 3, Table 5), we focused our attention on materials prepared with the SBA-15 support, *i.e.* {$R_3N^+Br^-$}@SBA-15 solids with {$Me_2EtN^+Br^-$}, {$MeEt_2N^+Br^-$}, {$Et_3N^+Br^-$} and {$Bu_3N^+Br^-$} groups. The catalytic tests were carried out at P_{CO2} = 10 bar, in a greener solvent, benzonitrile, with a higher SO:{$R_3N^+X^-$} molar ratio of 120 (0.8 mol%) at 120°C or even 80°C. Table **6** shows the results obtained after 3 h and 23 h of reaction. All the {$R_3N^+Br^-$}@SBA-15 materials tested afforded complete conversion of styrene oxide into styrene carbonate within 23 h at 120°C (Table 6, entries 3, 5, 7 and 9), unlike soluble Bu_4NBr alone (Table 6, entry 11). Although the yield of SC observed was already high after 3 h of reaction for all four catalysts (from 63 to 97%), it should be noted that the highest conversion values were obtained for ammonium with increased steric hindrance. Even if none of those catalysts allowed the completion of the reaction at 80°C, the same trend was actually observed whether after 3 h of reaction (from 16% with {$Me_2EtN^+Br^-$}@SBA-15 to 31% conversion with {$Bu_3N^+Br^-$}@SBA-15) or after 23 h (62 to 87%, Table 6, entries 4, 6, 8 and 10).

Of all the solids tested, {$Me_3N^+Cl^-$}@SBA-15 (entry 2, Table 6) is the only one that did not allow the complete conversion of styrene oxide at 120°C, even at longer time (only 40% after 23 h). Compared to all the materials investigated, {$Me_3N^+Cl^-$}@SBA-15 differs by the nature of the halide and the lowest steric hindrance of R substituents. Here, we believe that the low activity of {$Me_3N^+Cl^-$}@SBA-15 is mainly related to the formation of a stronger ion pair compared the other {$R_3N^+Br^-$}@SBA-15 materials tested. Despite the higher SO:{$R_3N^+X^-$} molar ratio used, improved activities of the {$R_3N^+Br^-$}@materials in benzonitrile compared to dichloromethane, could result from the use of a more dissociating solvent (ε = 25.9 vs. 8.9 for CH_2Cl_2) allowing the formation of loose anion/cation pairs. To explain the results, it is noteworthy that the solvation of bromide (and *a fortiori* of iodide) in benzonitrile is favored at the expense of harder chloride anions because of the potential formation of halide-π interactions[27] involving the phenyl group of benzonitrile.

Table 6: Catalytic performances of {$Bu_3N^+X^-$}@materials in CO_2 cycloaddition in benzonitrile

Entry	Catalysts	T (°C)	SC Yield	SC Yield

			after 3 h (%)	after 23 h (%)
1	SBA-15	120	0	0
2	{$Me_3N^+Cl^-$}@SBA-15	120	8	40
3	{$Me_2EtN^+Br^-$}@SBA-15	120	63	99
4	{$Me_2EtN^+Br^-$}@SBA-15	80	16	62
5	{$MeEt_2N^+Br^-$}@SBA-15	120	75	99
6	{$MeEt_2N^+Br^-$}@SBA-15	80	21	89
7	{$Et_3N^+Br^-$}@SBA-15	120	87	98
8	{$Et_3N^+Br^-$}@SBA-15	80	24	76
9	{$Bu_3N^+Br^-$}@SBA-15	120	97	99
10	{$Bu_3N^+Br^-$}@SBA-15	80	31	87
11	$Bu_4N^+Br^-$	120	62	84
12	$Bu_4N^+Br^-$	80	12	49

Benzonitrile (20 mL), P_{CO2} = 10 bar, p-xylene (8 mmol, internal standard), {$R_3N^+X^-$}@SBA-15 (corresponding to 0.045 mmol off QAS) and styrene oxide (0.665 mL, 5.6 mmol), leading to a SO:{ $R_3N^+X^-$} ratio of 120.

6.2.2. CO_2 cycloaddition onto SO in solvent-free conditions. The last set of experimental conditions tested did not involve any solvent. At first sight, this should avoid the use of potentially polluting organic solvents. However, it should be kept in mind that the catalyst separation step generally still requires solvents to allow filtration and/or extraction of the reaction products. From our point of view, the main advantage of such procedure is that it allowed to work with a higher substrate concentration. As a result, a much higher initial substrate/catalyst ratio was used. In the present study, this ratio was fixed at *ca.* 520 instead of 120 (SO: 31 mmol and X^-: 0.06 mmol, corresponding to *ca.* 0.2 mol% of catalyst). However, regarding the extended amount of SO used in this experiment, the quantity of CO_2 available needed to be also adapted, for a same volume of reactor. Under solvent-free conditions, the initial pressure of CO_2 was therefore fixed at 20 bar (corresponding to 32 mmol of CO_2) instead of 10 and the reaction time set at 6 h. It is noteworthy that in these conditions, the ratio CO_2:SO was thus slightly higher than 1. The results are presented in Table 7.

Table 7: Catalytic performances of {$Bu_3N^+X^-$}@materials and $Bu_4N^+Br^-$ in CO_2 cycloaddition in solvent-free conditions

Entry	Catalysts	SO Conv. (%)	SC Yield (%)
1	$Bu_4N^+Br^-$	37	35
2	$Bu_4N^+I^-$	44	43
3	{$Bu_3N^+Br^-$}@Zeosil	81	80

4	{$Bu_3N^+I^-$}@Zeosil	88	87
5	{$Bu_3N^+Br^-$}@SBA-15	84	83
6	{$Bu_3N^+I^-$}@SBA-15	80	80
7	{$Bu_3N^+Br^-$}@Zn/SBA-15	75	74
8	{$Bu_3N^+I^-$}@Zn/SBA-15	87	87
9	{$Bu_3N^+Br^-$}@KIT-6	62	62
10	{$Bu_3N^+I^-$}@KIT-6	75	73
11	{$Bu_3N^+Br^-$}@Zn/KIT-6	60	57
12	{$Bu_3N^+I^-$}@Zn/KIT-6	84	84

SO (31 mmol), LB= 0.194 mol% vs. SO (0.06 mmol), 100°C, 20 bar CO_2, 6 h.

All the tested catalysts gave better results in neat styrene oxide (table 7), than in CH_2Cl_2 at 100°C (Tables 4 and 5). As already mentioned for the tests in dichloromethane, also carried out for 6 h at 100°C (Table 5), the {$Bu_3N^+X^-$}@support catalysts (X = Br, I) (Table 7, entries 3-12) were more efficient compared to the soluble QAS (Table 7, entries 1-2). Moreover, very good catalytic activity was observed for all materials (Table 7, entries 3-12). In each case, the SO conversion (from 60 to 88%) as well as SC yield values (from 57 to 87%) obtained were systematically higher than those in CH_2Cl_2 (see Table 5). It is noteworthy that the effects of the nature of the halogen anion (bromide *vs.* iodide) and of the presence of Zn^{2+} ions in the materials were similar in solvent and solvent-free conditions. A slightly improved SC yield was observed for the SBA-15 and KIT-6 materials containing zinc cations (Table 7, entries 6 *vs.*8 and entries 10 *vs.*12) and in general the iodide containing materials are more efficient than their bromide analogs, except for {Bu_3NBr}@SBA-15 (Table 7, entry 5). Even if the latter material gave superior results in CH_2Cl_2 or benzonitrile, this was not observed in solvent-free conditions, where the iodide containing zinc {Bu_3NI}@Zn/SBA-15 gave the best SC yield (Table 7, entry 8).

6.3 Recycling ability of {$Bu_3N^+Br^-$}@SBA-15. Recycling tests of the catalysts were performed in solvent-free conditions, choosing {$Bu_3N^+Br^-$}@SBA-15 as a model. The latter was evaluated over five runs (Figure 4), recovering the catalyst from the reaction mixture and washing it before next run, as detailed in the experimental section (paragraph 4.4). The amount of styrene oxide re-engaged was calculated for each run, in order to keep the same ratio of bromide *vs.* styrene oxide, assuming that the catalyst would preserve the same halogen loading.

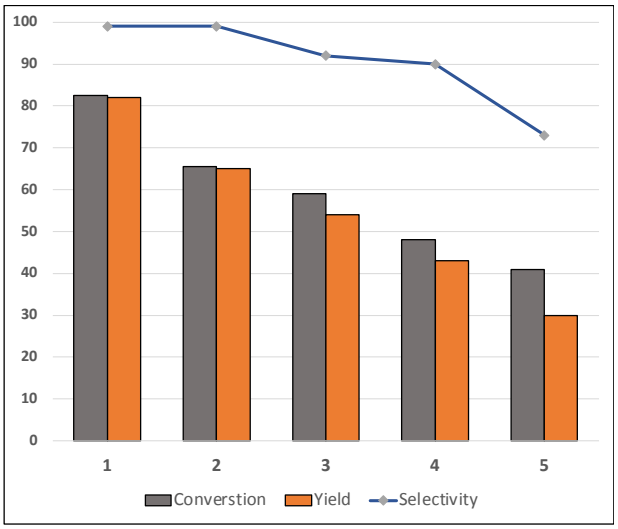

Figure 4. Recycling experiment using {$Bu_3N^+Br^-$}@SBA-15 over five runs in solvent-free conditions.

Reaction conditions: SO (31 mmol),{$Bu_3N^+Br^-$}@SBA-15 *(0.2 mol% vs SO, 0.06 mmol), 100°C, 20 bar CO_2, 6 h.*

It turned out that the catalytic activity decreased progressively after each cycle, leading to lower SO conversion and lower cyclic carbonate selectivity, in particular for the latter run. This observation could be related to the lixiviation of the QAS bromide or to the progressive exchange of bromides by other anions in the reaction conditions. The catalyst recovered from the fifth run was analyzed by thermogravimetric analysis (TGA) and solid-state ^{13}C NMR spectroscopy in order to get some information to understand this loss of catalytic activity.

TG analysis of the {$Bu_3N^+Br^-$}@SBA-15 catalyst after five runs was carried out and its results compared to those obtained with the fresh catalyst i) as it was engaged in the first run and ii) after being subjected to intensive washing (8 x 10 mL CH_2Cl_2) mimicking the successive treatments one the used catalyst. As shown in Figure 5a, the fresh and intensively washed catalysts provided similar TGA curves, pointing out that intensive washing did not cause any significant lixiviation. Nevertheless, the curve corresponding to the recycled catalyst was different from that measured with the starting material. Therefore, it can be stated that the catalyst underwent some evolution during the five successive runs, which is reflected on the curve by the absence of a clearly defined plateau, unlike what was observed for the fresh sample or after intensive washing. There is clearly a loss of homogeneity in the organic part. Furthermore, these results suggest that there was an overall loss of mass slightly greater than that observed for the fresh sample. The comparison of the derivative functions of the TGA curves were also instructive as shown in Figure 5b. As expected, the fresh and washed

catalysts were characterized by similar derivative curves. On the contrary, the derivative curve plotted for the five times recycled catalyst was more complex, since emphasizing more components, especially in the range of 150 to 450°C.

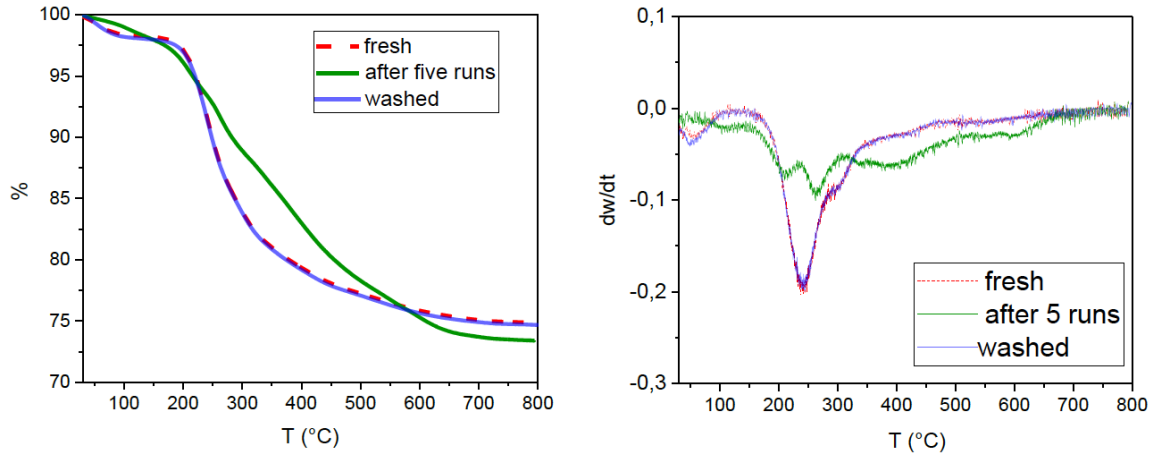

Figure 5: TGA curves (a) and their derivatives (b) for the fresh, recycled after five runs and intensively washed {$Bu_3N^+Br^-$}@SBA-15.

The fresh catalyst and the material recovered after 5 runs were analyzed by solid-state ^{13}C NMR (Figure 6), in order to try to identify the nature of the organic molecules participating to the catalyst deactivation. For the fresh materials, the main peaks 1 to 4 were attributed to butyl chains of the ammonium, while the two less intense peaks (6 and 7) were assigned to the carbon atoms connected to the silicon atom. Even if all these peaks could be observed on the spectrum of the recycled catalyst, intense additional signals were also present, especially between 70 and 150 ppm. These additional peaks were attributed to the presence of poly(styrene oxide) (or PSO) resulting from the ring-opening polymerization of styrene oxide.[28] Therefore, it is likely that PSO could impregnate the surface of the silica, poisoning the catalyst and limiting the catalytic performances of the QAS grafted at the surface of the silica. If we look closely at the ATG results, it appears that the mass loss observed between 200 and 700°C is fairly close in the initial material and the recycled material. If we compare this with the ^{13}C solid state NMR results, it appears that, since the NMR shows the adsorption of polymers in large quantities on the support, mechanically the quantity of ammonium grafts still present on the support must therefore be much lower on the recycled catalyst. In summary, if we analyze NMR and TGA data in parallel, it appears that:

- the mass loss observed between 200 and 700°C in TGA was fairly close in the initial and the recycled materials. However, the TG profiles *vs.* temperature of both samples are significantly different.

- ^{13}C solid state NMR results showed the adsorption of polymers in large quantities on the support.

The conclusion of these two studies is that, mechanically, the quantity of ammonium grafts still present on the support must therefore be lower on the recycled catalyst. According to these results, we can assume that some leaching of the catalyst occured, even if the subsequent NMR studies also show that this phenomenon is compounded by the formation of poly(styrene oxide).

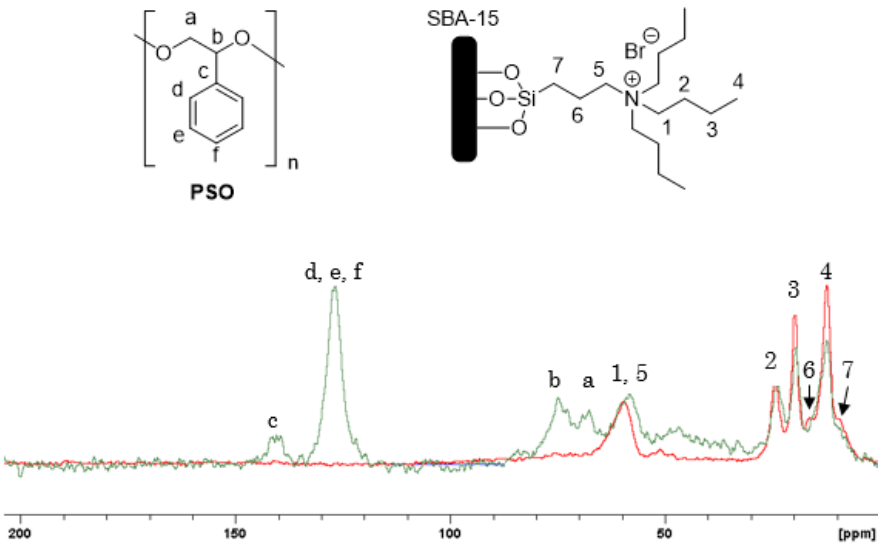

Figure 6. Solid-state ^{13}C NMR spectra of fresh {$Bu_3N^+Br^-$}@SBA-15 catalyst (red) and after five runs (green).

CONCLUSION. In this work, materials bearing ammonium halides moieties were synthesized by covalently grafting silylated QAS onto several silica supports with different pore arrangements (SBA-15, KIT-6) as well as using commercial Zeosil or Aerosil R812. Zn^{2+}-doped support analogs (Zn/SBA-15 and Zn/KIT-6) were also prepared in order to determine the effect of the introduction of an external Lewis acid. In this regard, silylated QAS with different size chains (from trimethyl to tributylammonium derivatives) and different associated halides (Cl, Br and I) were used, leading to the preparation of a wide series of catalysts. The performances of all materials, including the unfunctionalized supports, were evaluated in the

CO_2 cycloaddition into styrene oxide (SO) to form cyclic styrene carbonate (SC), using three sets of conditions. Different parameters were thus studied in the course of this work allowing to draw some general conclusions.

- Addition of a silica support in the presence of a soluble QAS systematically provided a benefit in terms of both SO conversion and SC yield, whatever the pore structure of the support. It seems that the most important parameter is the number of Si-OH functions brought by the support, these last playing the role of additional Lewis acid co-catalysts. This was also confirmed by the use of a partially methylated silica support which significantly lowered the catalytic performances of the corresponding materials.
- Covalent grafting of quaternary ammonium halides did not reduce their catalytic activity compared with conditions where soluble QAS such as NBu_4X (X = Cl, Br, I) are associated with the naked supports. The main added benefit of their immobilization is therefore in terms of catalyst separation.
- Addition of Zn^{2+} ions in the framework of the silica had no tremendous effect on the catalytic activity, the Lewis acid role of zinc cations being negligible compared to the one of the Si-OH groups.
- As expected, the carbon chain lengths of the QAS are key parameters to improve the catalytic activity of the materials: QAS hindered by longer chains led to higher catalytic activity increasing both SO conversion and SC yield.
- Solvents with high permittivity such as benzonitrile only allowed to emphasize differences between the halides borne by the supported QAS. In that case, it could be shown that the order of efficiency is as follows: Cl < Br ≈ I.
- Solvent-free conditions were tested successfully, affording up to 80% yield of styrene carbonate within 6 h at 100°C with *ca*. 0.2 mol% of catalyst. However recyclability has to be improved, since lixiviation of the catalyst was observed. Indeed, $\{Bu_3N^+Br^-\}$@SBA-15) taken as an example, exhibited a loss of SC yield of about 65% after five runs. Unfortunately, solvent-free conditions seem also to favor side polymerization of the epoxide forming poly(styrene oxide) as suggested by solid-state ^{13}C NMR. Here the use of a lower pressure, while keeping stoichiometric conditions, could be envisaged by working with an equipment delivering CO_2 on demand.

- With $\{Bu_3N^+Br^-\}$@SBA-15, the catalytic test performed in benzonitrile at 0.8 mol% of QAS at 80°C for 3 h under 10 bar of CO_2 displayed a TOF of c.a. 40 h^{-1}, that run at 0.2 mol% of QAS without solvent at 100°C for 6 h under 20 bar of CO_2 a TOF of c.a. 54 h^{-1}, while that performed in dichloromethane at 3 mol% of QAS at 100°C for 6 h under 10 bar of CO_2 gave a TOF value of c.a. 3 h^{-1}.

Conflicts of interest

There are no conflicts to declare.

Acknowledgements

This study benefited from the support of the project OxCyCat-CO_2 ANR-17-CE06-0009 of the French Agence Nationale de la Recherche (ANR) for the PhD fellowships to Mr Miguel Alonso de la Peña and Mr Matthieu Balas, for the grant of Mrs Julie Kong, and more generally for funding this work. The authors want also to acknowledge the Centre National de la Recherche Scientifique (CNRS), Claude Bernard Lyon 1 University and Sorbonne Université.

[1] a) Global Carbon Budget 2022. P. Friedlingstein and co- workers, *Earth Syst. Sci. Data* 2022, 14, 4811–4900. b) Growth in emission transfers via international trade from 1990 to 2008. G. P. Peters, J. C. Minx, C.L. Weber and O. Edenhofer, *PNAS*, 2011, **108**, 8903-8908.

[2] How much carbon dioxide can we emit? P. Glen, 2017, Published online at https://www.cicero.oslo.no/en/posts/climate-news/how-much-carbon-dioxide-can-we-emit, CICERO.

[3] CO_2 and Greenhouse Gas Emissions. H. Ritchie, M. Roser and P. Rosado, 2020, Published online at https://ourworldindata.org/co2-and-greenhouse-gas-emissions.

[4] Captage et stockage du gaz carbonique (CSC). B. Durand, NCL Collect. Store. 2011, 1–32. Published online at https://inis.iaea.org/collection/NCLCollectionStore/_Public/43/009/43009426.pdf.

[5] Carbon capture and storage (CCS): the way forward. M. Bui, C. S. Adjiman, A. Bardow, E. J. Anthony, A. Boston, S. Brown, P. S. Fennell, S. Fuss, A. Galindo, L. A. Hackett, J. P. Hallett, H. J. Herzog, G. Jackson, J. Kemper, S. Krevor, G. C. Maitland, M. Matuszewski, I. S. Metcalfe, C. Petit, G. Puxty, J. Reimer, D. M. Reiner, E. S. Rubin, S. A. Scott, N. Shah, B. Smit, J. P. Martin Trusler, P.l Webley, J. Wilcox and N. Mac Dowell, *Energy Environ. Sci.*, 2018, **11**, 1062-1176

[6] Carbon dioxide utilization in the chemical industry. M. Aresta and I. Tommasi, *Energy Convers. Manag.*, 1997, **38**, 373–378.

[7] a) The changing paradigm in CO_2 utilization. M. Aresta, A. Dibenedetto and A. Angelini*, J. CO2 Util.*, 2013, **3–4**, 65–73. b) Special Issue: Catalysis for CO_2 conversion, *ChemSusChem*, 2017, **10**, 1034-1297.

[8] a) Enzymic versus chemical carbon dioxide utilization. Part I. The role of metal centers in carboxylation reactions. M.Aresta, E. Quaranta, I. Tommasi, P. Giannoccaro and A. Ciccarese, *Gazz. Chim. Ital.*, 1995, **125**, 509–538. b) What would it take for renewably powered electrosynthesis to displace petrochemical processes? P. De Luna, C. Hahn, D. Higgins, S. A. Jaffer, T. F. Jaramillo and E. H. Sargent, *Science*, 2019, **364,** eaav3506. c) Homogeneously Catalyzed Electroreduction of Carbon Dioxide—Methods, Mechanisms, and Catalysts, R. Francke, B. Schille and M. Roemelt, *Chem. Rev.*, 2018, **118**, 4631–4701.

[9] a) Making Plastics from Carbon Dioxide: Salen Metal Complexes as Catalysts for the Production of Polycarbonates from Epoxides and CO_2. D. Darensbourg, *Chem. Rev.,* 2007, **107**, 2388-2410. b) Synthesis of cyclic carbonates from epoxides and CO_2. M. North, R. Pasquale and C. Young, *Green Chem.*, 2010, **12**, 1514-1539. c) Recent Advances in the Catalytic Preparation of Cyclic Organic Carbonates. C. Martin, G. Fiorani and A. W. Kleij, *ACS Catal.*, 2015, **5**, 1353-1370. d) CO_2-fixation into cyclic and polymeric carbonates: principles and applications. A. J. Kamphuis, F. Picchioni and P. P. Pescarmona,

Green Chem., 2019, **21**, 406-448. e) Chromium-salophen as a soluble or silica-Supported co-catalyst for the fixation of CO_2 onto styrene oxide at low temperatures. M. Balas, L. K/Bidi, F. Launay and R. Villanneau, *Front. Chem.*, 2021, **9**, 765108.

[10] Bibliographic survey of the strategies implemented for the one-pot synthesis of cyclic carbonates from styrene and other alkenes using CO_2 and green oxidants. M. Balas, R. Villanneau and F. Launay, *J. CO_2 Util.*, 2022, **65**, 102215.

[11] Challenges in the catalytic synthesis of cyclic and polymeric carbonates from epoxides and CO_2. P. P. Pescarmona and M. Taherimehr, *Catal. Sci. Technol.*, 2012, **2**, 2169-2187.

[12] New zinc/tetradentate N_4 ligand complexes: Efficient catalysts for solvent-free preparation of cyclic carbonates by CO_2/epoxide coupling. I. Karamé, S. Zaher, N. Eid and L. Christ, *Mol. Catal.*, 2018, **456**, 87-95.

[13] Synergistic hybrid catalyst for cyclic carbonate synthesis: Remarkable acceleration caused by immobilization of homogeneous catalyst on silica. T. Takahashi, T. Watahiki, S. Kitazume, H. Yasuda and T. Sakakura, *Chem. Commun.*, 2006, 1664–1666.

[14] Silylated quaternary ammonium salts – ionic liquids with hydrophobic cations, M. Kozelj, A. Guerfi and K. Zaghib, *J. Mater. Chem. A*, 2014, **2**, 15964-15971.

[15] Morphological Control of Highly Ordered Mesoporous Silica SBA-15. D. Zhao, J. Sun, Q. Li and G. D. Stucky, *Chem. Mater.*, 2000, **12**, 275–279.

[16] a) Cubic Ia3d large mesoporous silica: synthesis and replication to platinum nanowires, carbon nanorods and carbon nanotubes. F. Kleitz, S. H. Choi and R. Ryoo, *Chem. Commun.*, 2003, 2136-2137. b) MCM-48-like Large Mesoporous Silicas with Tailored Pore Structure: Facile Synthesis Domain in a Ternary Triblock Copolymer−Butanol−Water System. T. W. Kim, F. Kleitz, B. Paul and R. Ryoo, *J. Am. Chem. Soc.*, 2005, **127**, 7601–7610.

[17] Design of bifunctional NH_3I-Zn/SBA-15 single-component heterogeneous catalyst for chemical fixation of carbon dioxide to cyclic carbonates. M. Liu, B. Liu, L. Liang, F. Wang, L. Shi and J. Sun, *J. Mol. Catal. A Chem.*, 2016, **418-419**, 78-85.

[18] Mesostructured Au/C materials obtained by replication of functionalized SBA-15 silica containing highly dispersed gold nanoparticles. F. Kerdi, V. Caps and A. Tuel, *Microporous Mesoporous Mater.*, 2011, **140**, 89–96.

[19] a) Silica-supported aminopyridinium halides for catalytic transformations of epoxides to cyclic carbonates under atmospheric pressure of carbon dioxide. K. Motokura, S. Itagaki, Y. Iwasawa, A. Miyaji and T. Baba, *Green Chem.*, 2009, **11**, 1876-1880. b) Synthesis of Cyclic Carbonates from Epoxides and Carbon Dioxide by Using Organocatalysts. M. Cokoja, M.E. Wilhelm, M.H. Anthofer, W.A. Herrmann and F.E. Kühn, *ChemSusChem*, 2015, **8**, 2436-2454. c) Synthesis of Propylene Carbonate on a Bifunctional Titanosilicate Modified with Quaternary Ammonium Halides. J. Zhang, Y. Liu, N. Li, H. Wu, X. Li, W. XIE, Z. Zhao, P. Wu and M. He, *Chinese J. Catal.*, 2008, **29**, 589-591.

[20] Immobilization of ionic liquid on hybrid MCM-41 system for the chemical fixation of carbon dioxide on cyclic carbonate. S. Udayakumar, S.-W. Park, D.-W. Park and B.-S. Choi, *Catal. Commun.*, 2008, **9**, 1563–1570.

[21] Physisorption of gases, with special reference to the evaluation of surface area and pore size distribution (IUPAC Technical Report). M. Thommes, K. Kaneko, A. V Neimark, J. P. Olivier, F. Rodriguez-Reinoso, J. Rouquerol and K. S. W. Sing, *Pure Appl. Chem.*, 2015, **87**, 1051-1069.

[22] a) Covalent grafting of organic–inorganic polyoxometalates hybrids onto mesoporous SBA-15: a key step for new anchored homogeneous catalysts. R. Villanneau, A. Marzouk, Y. Wang, A. Ben Djamaa, G. Laugel, A. Proust and F. Launay, *Inorg. Chem.*, 2013, **52**, 2958-2965. b) Advantages of covalent immobilization of metal-Salophen on amino-functionalized mesoporous silica in terms of recycling and catalytic activity for CO_2 cycloaddition onto epoxides. M. Balas, S. Beaudoin, A. Proust, F. Launay and R. Villanneau, *Eur. J. Inorg. Chem.*, 2021, 1581-1591.

[23] Handbook of X-ray Photoelectron Spectroscopy, C. D. Wagner, W. M. Riggs, L. E. Davis and J. F. Moulder, *ed.* G. E. Muilenberg, Perkin–Elmer Corporation, Eden Prairie, MN, USA, 1978.

[24] a) Synergistic hybrid catalyst for cyclic carbonate synthesis: Remarkable acceleration caused by immobilization of homogeneous catalyst on silica, T. Takahashi, T. Watahiki, S. Kitazume, H. Yasuda and T. Sakakura, *Chem. Commun*., 2006, 1664-1666. b) Supported imidazole as heterogeneous catalyst for the synthesis of cyclic carbonates from epoxides and CO_2, M. Sankar, T. G. Ajithkumar, G. Sankar and P. Manikandan, *Catal. Commun.*, 2015, **59**, 201-205. c) Heterogeneous catalysts for cyclic carbonate synthesis from carbon dioxide and epoxides, A. A. Marciniak, K. J. Lamb, L. P. Ozorio, C. J. A. Mota and M. North, *Curr. Opin. Green Sustain. Chem.*, 2020, **26**, 100365.

[25] Robust pyrrole-Schiff base Zinc complexes as novel catalysts for the selective cycloaddition of CO_2 to epoxides, M. Alonso de la Pena, L. Merzoud, W. lamine, A. Tuel, H. Chermette and L. Christ, *J. CO_2 Util.*, 2021, **44**, 101380.

[26] Sanofi's solvent selection guide: a step toward more sustainable processes. D. Prat, O. Pardigon, H-W. Flemming, S. Letestu, V. Ducandas, P. Isnard, E. Guntrum, T. Senac, S. Ruisseau, P. Cruciani and P. Hosek, *Org. Process Res. Dev.*, 2013, **17**, 1517−1525

[27] a) Counterintuitive interaction of anions with benzene derivatives. D. Quinonero, C. Garau, A. Frontera, P. Ballester, A. Costa and P. M. Deya, *Chem Phys Lett*., 2002, **359**, 486-492. b) Anion–π Interactions: Do They Exist? D. Quinonero, C. Garau, C. Rotger, A. Frontera, P. Ballester, A. Costa and P. M. Deya., *Angew. Chem. Int. Ed*., 2002, **41**, 3389-3392.

[28] Synthesis of poly(styrene oxide) with different molecular weights using tin catalysts. A. Kayan, *Des. Monomers Polym.*, 2015, **18**, 545–549.